

## RESEARCH ARTICLE

# Dynamic soaring decouples dynamic body acceleration and energetics in albatrosses

Melinda G. Conners<sup>1,2,\*</sup>, Jonathan A. Green<sup>3</sup>, Richard A. Phillips<sup>4</sup>, Rachael A. Orben<sup>5</sup>, Chen Cui<sup>6</sup>, Petar M. Djurić<sup>6</sup>, Eleanor Heywood<sup>1</sup>, Alexei L. Vyssotski<sup>7</sup> and Lesley H. Thorne<sup>1</sup>

## ABSTRACT

Estimates of movement costs are essential for understanding energetic and life-history trade-offs. Although overall dynamic body acceleration (ODBA) derived from accelerometer data is widely used as a proxy for energy expenditure (EE) in free-ranging animals, its utility has not been tested in species that predominately use body rotations or exploit environmental energy for movement. We tested a suite of sensor-derived movement metrics as proxies for EE in two species of albatrosses, which routinely use dynamic soaring to extract energy from the wind to reduce movement costs. Birds were fitted with a combined heart-rate, accelerometer, magnetometer and GPS logger, and relationships between movement metrics and heart rate-derived  $\dot{V}_{O_2}$ , an indirect measure of EE, were analyzed during different flight and activity modes. When birds were exclusively soaring, a metric derived from angular velocity on the yaw axis provided a useful proxy of EE. Thus, body rotations involved in dynamic soaring have clear energetic costs, albeit considerably lower than those of the muscle contractions required for flapping flight. We found that ODBA was not a useful proxy for EE in albatrosses when birds were exclusively soaring. As albatrosses spend much of their foraging trips soaring, ODBA alone was a poor predictor of EE in albatrosses. Despite the lower percentage of time flapping, the number of flaps was a useful metric when comparing EE across foraging trips. Our findings highlight that alternative metrics, beyond ODBA, may be required to estimate energy expenditure from inertial sensors in animals whose movements involve extensive body rotations.

**KEY WORDS:** Energy expenditure, Movement costs, Accelerometry, Angular velocity, ODBA, Flight efficiency

## INTRODUCTION

Wide-ranging animals have evolved various physical and behavioral mechanisms for reducing costs of movement, including morphological adaptations for particular modes of locomotion and the use of environments that optimize travel efficiency (Duriez et al., 2014;

Milner-Gulland et al., 2011; Saadat et al., 2017). Nevertheless, travel costs are a major component of daily energy budgets, and drive many facets of physiology and ecology. Thus, factors that influence the energetics of travel, such as resource abundance and distribution, predator avoidance, weather and other environmental conditions, also affect reproduction and survival (Booksmythe et al., 2008; Gallagher et al., 2017; Wall et al., 2006). Quantifying movement costs is therefore critical for understanding the biological and ecological drivers of life history.

Over the past decade, miniaturized accelerometers deployed on free-ranging animals have dramatically improved our ability to study energetics *in situ* (Wilmers et al., 2015). Three-dimensional acceleration recorded at high resolution (typically 10–60 Hz) allows for instantaneous body movements to be measured continuously. These data are often used to identify behaviors (Nathan et al., 2012; Shepard et al., 2008; Yoda et al., 1999), and to derive movement metrics that serve as proxies of energy expenditure, such as flipper strokes, tail beats or wing beats per unit time (Gleiss et al., 2009; Jeanniard-du-Dot et al., 2016; Usherwood et al., 2011). Additionally, overall dynamic body acceleration (ODBA), a metric of integrated body acceleration across three orthogonal axes, has emerged as a versatile proxy for energy expenditure, improving our understanding of activity-specific costs across a wide spectrum of free-ranging animals (Green et al., 2009; Halsey et al., 2009, 2011; Wilson et al., 2006, 2020).

The conceptual underpinning of ODBA is that acceleration of a body is the result of force exerted by muscle, and that the rate of oxygen consumption ( $\dot{V}_{O_2}$ ), an indirect measure of energy expenditure, is proportional to this force (Cavagna et al., 1963). Numerous animal and human experiments have validated this general relationship by directly measuring  $\dot{V}_{O_2}$  in active individuals fitted with accelerometers (Gleiss et al., 2011; Halsey et al., 2008). However, the correlation between ODBA and  $\dot{V}_{O_2}$  is highly dependent on study design and is influenced by environmental factors such as temperature (e.g. within versus outside the thermal neutral zone; Halsey et al., 2011) and intrinsic characteristics such as body size (Martin Lopez et al., 2022). Moreover, ODBA is subject to errors associated with changes in acceleration that are independent of muscle-powered movement, a constraint which has received little attention to date (Wilson et al., 2020). For example, some animals gain kinetic energy from the environment that manifests as dynamic body acceleration, but without the associated mechanical cost of muscle contraction. Wilson et al. (2020) called this ‘environmental DBA’ and highlighted a study by Gómez Laich et al. (2011) that recorded a striking increase in dynamic body acceleration in imperial cormorants *Leucocarbo atriceps* resting on the water in high sea states.

The greatest potential to extract environmental energy for transport occurs in animals that swim or fly by exploiting variability in fluid flow (Chapman et al., 2011). These include birds that use energy from

<sup>1</sup>School of Marine and Atmospheric Sciences, Stony Brook University, NY 11794-5000, USA. <sup>2</sup>Western EcoSystems Technology, Inc., 415 West 17th Street, Cheyenne, WY 82001, USA. <sup>3</sup>School of Environmental Sciences, University of Liverpool, Liverpool L69 3GP, UK. <sup>4</sup>British Antarctic Survey, Natural Environment Research Council, High Cross, Madingley Road, Cambridge CB3 0ET, UK. <sup>5</sup>Department of Fisheries, Wildlife, and Conservation Sciences, Oregon State University, Hatfield Marine Science Center, 2030 SE Marine Science Dr., Newport, OR 97365, USA. <sup>6</sup>Department of Electrical and Computer Engineering, Stony Brook University, NY 11794-5000, USA. <sup>7</sup>Institute of Neuroinformatics, University of Zurich and Swiss Federal Institute of Technology (ETH), Zurich 8057, Switzerland.

\*Author for correspondence (mconners@west-inc.com)

 M.G.C., 0000-0003-0572-0026; L.H.T., 0000-0002-6297-0091

a wind-shear gradient at the ocean–atmospheric boundary in a flight pattern called dynamic soaring (Wilson, 1975; Pennycuik, 1982; Fig. 1A). Dynamic soaring is considered one of the most efficient forms of travel (Pennycuik, 1982), and primarily occurs in the procellariiform seabirds, particularly albatrosses, shearwaters and other petrels. During dynamic soaring, birds experience high speeds concomitant with rapid gains and losses in acceleration as they climb and descend the wind-shear gradient (Bousquet et al., 2017). In contrast, birds such as raptors that soar by exploiting thermal lift (i.e. thermal soaring) do not experience marked changes in acceleration (Duriez et al., 2014; Williams et al., 2015). Hence, while both thermal soaring raptors and dynamic soaring seabirds move with minimal mechanical work by exploiting environmental energy, ODBA is likely higher in the latter as a result of the cyclical accelerations experienced by the bird when ascending and descending the wind-shear gradient. Given that proxies of energy expenditure have not been assessed relative to dynamic soaring behavior within foraging trips, there is a need to understand the relationship between soaring movements, ODBA and energy expenditure.

In addition to the challenge of distinguishing acceleration generated by the environment, ODBA may not capture all acceleration generated by the animal, particularly those subjected to *g*-force in fast maneuvers such as cornering cheetahs *Acinonyx jubatus* or stooping and banking birds (Williams et al., 2015; Wilson et al., 2020). Here, the costs of movement may be better represented by other metrics. For example, VeSBA, the vectorial norm of static body acceleration, can be used to measure inertial acceleration from fast movements that induce centripetal forces on the animal (Williams et al., 2015, 2013a, 2020). Given the characteristic sharp banking angles and high speeds of dynamic soaring birds, VeSBA may better capture power-generated movements, but the relationship between VeSBA and energy expenditure has yet to be explored.

Turning costs also contribute to the energetics of travel (Wilson et al., 2013a), and these rotational movements may also be more effectively measured by alternative metrics. ODBA was found to chronically underestimate the cost of movement in large aquatic species, which was attributed to the greater contribution of rotational movement to acceleration of larger animals (Martin Lopez et al., 2022). Sensors that are not sensitive to centripetal acceleration and can be used to measure body rotations, such as magnetometers and gyroscopes, enable additional, novel metrics to be evaluated (Williams et al., 2017). Angular velocity metrics derived from accelerometer and magnetometer data describe high-resolution rotational activity (Gunner et al., 2020, 2021). These may better reflect energetic costs in dynamic soaring birds given the demonstrated costs of body rotation in other species (Wilson et al., 2013b).

Albatrosses have evolved a number of anatomical features to reduce energetic costs while soaring, such as long, narrow wings (high aspect ratio), a shoulder-locking mechanism to reduce the effort of wing extension, and an extensive network of slow-twitch musculature that likely powers postural holds through static, isometric contractions (Meyers and Stakebake, 2005). However, energy efficient, dynamic soaring must still incur energetic costs, given the involvement of slow-twitch muscles in wing extension, the postural changes required to maintain aerodynamic stability in strong winds, and the turning costs associated with the characteristic steep-banking maneuvers. As dynamic soaring can comprise up to 96% of flight time in albatrosses (Sakamoto et al., 2013), it is important to identify factors that drive variability in the associated energetic costs of soaring, and those of other flight modes such as

flapping, to quantify the overall cost of transport. The relatively high cost of flapping versus dynamic soaring in albatrosses is based on theoretical models (Pennycuik, 2008), studies that have measured mean energy expenditure across entire foraging trips (Adams et al., 1986; Costa and Prince, 1987; Shaffer, 2011) and studies using heart-rate loggers (Sakamoto et al., 2013; Weimerskirch et al., 2000); however, these were limited by small sample sizes, coarse sampling resolution, or flight behavior that was inferred, rather than measured directly. Thus, further exploration of the energetic consequences of these two flight modes using fine-scale data from within foraging trips is needed to better understand movement efficiency and energetic tradeoffs in the flight of albatrosses and other procellariiform seabirds.

Here, we assessed the utility of a suite of metrics commonly derived from accelerometers and novel metrics from magnetometers that capture characteristics of dynamic soaring flight as proxies of energy expenditure during flight in seabirds. We focused on two species that use dynamic soaring and flapping flight, the black-browed albatross *Thalassarche melanophris* (Temminck 1828) and the grey-headed albatross *Thalassarche chrysostoma* (Forster 1785), to evaluate the costs and benefits of different flight modes at sea. Our specific objectives were to: (1) determine fine-scale time budgets during foraging trips and assess how proxies of energy expenditure vary with flight mode; (2) evaluate different metrics derived from accelerometers as potential proxies of energy expenditure at different temporal scales; and (3) test whether characteristics of dynamic soaring (soaring arc magnitude and arc rate) or metrics associated with postural change (VeSBA) offer advantages over ODBA in explaining variability in energy expenditure when birds are engaged exclusively in dynamic soaring.

## MATERIALS AND METHODS

### Instruments

To capture high-resolution movement and heart-rate data from albatrosses foraging at sea, we deployed a specialized biologging device (Neurologger 2A, Evolocus, NY, USA) that contained multiple sensors in a single enclosed unit. The single enclosed unit contained a miniaturized 600 Hz electrocardiogram (ECG) recorder ( $\pm 6$  mV, 10-bit), 75 Hz triaxial accelerometer (LSM6DSOX,  $\pm 16$  g, 16-bit), 75 Hz triaxial magnetometer (IIS2MDC,  $\pm 49$  Gauss, 16-bit), and GPS unit (Cat-logger, Perthold Engineering LLC, Anderson, SC, USA, set to record at 2 min intervals), powered by a rechargeable lithium-ion battery (2600 mAh, 3.6 V, 18650) and writing to a 2 GB flashchip. The device was sealed in polyolefin heat-shrink tubing (25.4 mm diameter, 0.9 mm thickness), and further water-proofed by hot glue. The dimensions of the device were approximately 18×18×70 mm, and the total mass, including tape and heat shrink, ranged from 64 to 67 g, which was on average 2.1% of bird mass ( $\pm 0.3\%$ , range 1.7–3.1%). The device mass (including tape) only exceeded 3.0% in a single bird, which was something of an anomaly. Excluding that bird, the next largest percentage was 2.5%; thus, the majority of devices were below the threshold where device effects can become apparent in pelagic seabirds (Phillips et al., 2003).

### Device deployments

Devices were deployed at Bird Island, South Georgia (54°00'S, 38°03'W) from November 2019 to February 2020 on black-browed and grey-headed albatrosses during the incubation and brood-guard stages. Grey-headed albatrosses are marginally smaller than black-browed albatrosses in most body dimensions but have slightly higher wing loadings and aspect ratios (Phillips et al., 2004), and

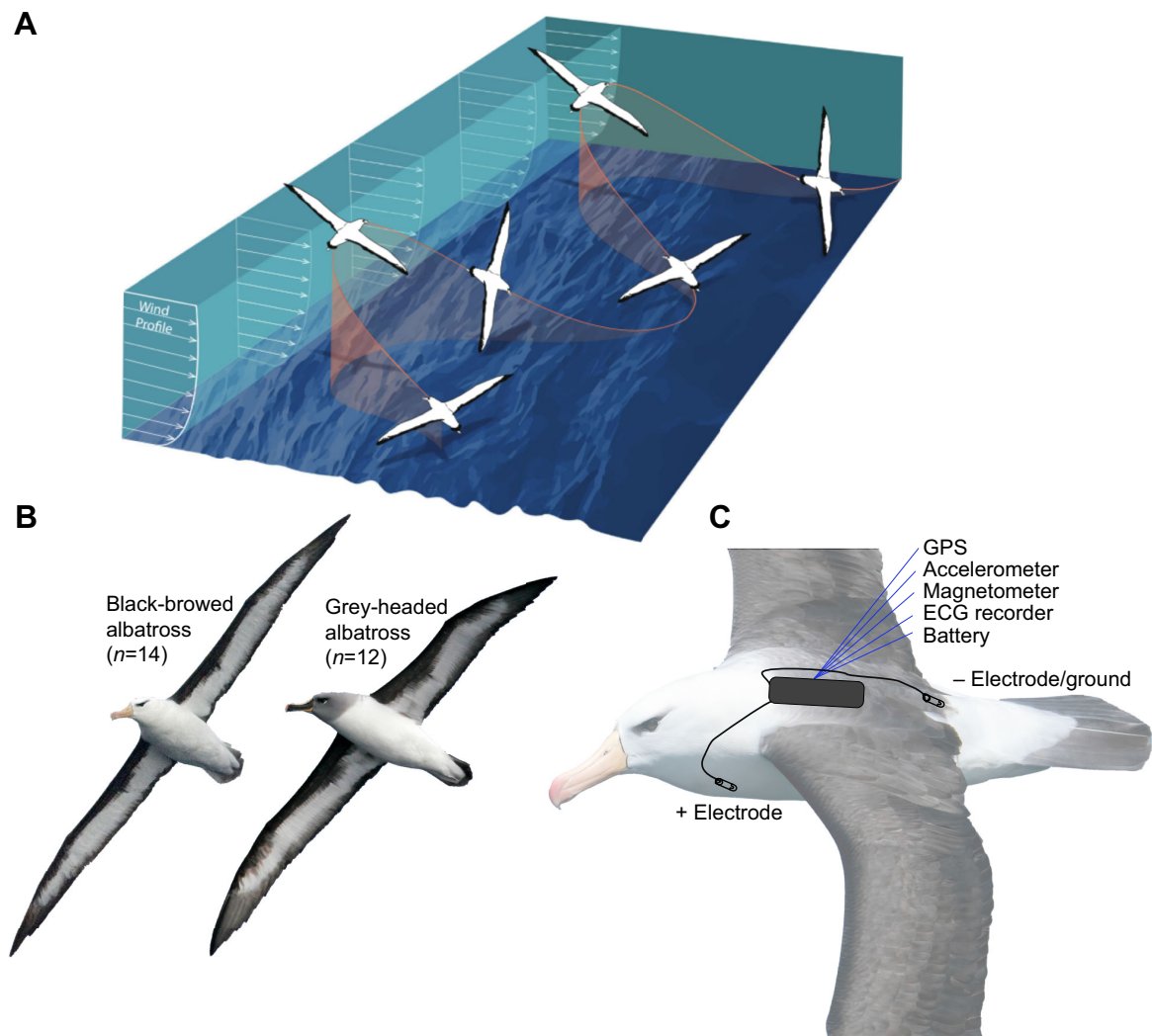


**Fig. 1. An overview of the dynamic soaring flight mode, study species and device attachment.** (A) A schematic diagram showing dynamic soaring behavior in the albatross. During dynamic soaring, albatrosses fly into the wind, decelerate while gaining altitude, then turn at the peak altitude into the direction of the wind, where the bird descends and gains acceleration (illustration from Richardson et al., 2018, Springer Nature Group, reproduced under the terms of the Creative Commons CC BY license). This form of flight is highly periodic and requires changes in body position (e.g. banking, heading) rather than dynamic movements of the bird's wings. (B) The two study-species, black-browed and grey-headed albatrosses, are similar in shape and size, both species having the long narrow wings and high aspect ratios characteristic of birds that perform dynamic soaring flight. (C) An illustration of the back attachment of the heart rate ( $f_H$ ) logger and electrodes.

tend to forage in regions with higher wind velocities (Phillips et al., 2004; Wakefield et al., 2009). Just prior to departing on a foraging trip, breeding albatrosses were captured at the nest and weighed to the nearest 50 g with a Pesola spring balance. The biologging device was attached to the central mantle feathers using Tesa tape (#4651, Tesa, Norderstedt, Germany). The tag frame (described by the  $x$ ,  $y$  and  $z$  axes) was aligned with the anterior–posterior (surge), medio-lateral (sway) and dorsal–ventral (heave) axes of the bird (the ‘bird frame’; Fig. 1C). Single insulated wires (26 gauge, ~7–10 cm long) exited from the front and rear of the waterproof casing, the terminal ends of which were attached to an electrode (25 mm nickel-plated safety pin). These electrodes were attached subcutaneously, one a few centimeters below the top of the left shoulder and the other on the lower right back. Safety pins were replaced before every deployment and the skin disinfected with 70% alcohol prior to insertion. Black-browed and grey-headed albatrosses are sexually dimorphic and were sexed using morphometric measurements (Phillips et al., 2004).

Devices were deployed on 14 black-browed albatrosses and 12 grey-headed albatrosses, and recorded 1360 and 1275 h, respectively (total 2635 h) of accelerometer, magnetometer and ECG data. All high-resolution ECG, accelerometer and magnetometer data were pre-processed, analyzed and visualized in Matlab (2019a) using functions from the Animal Tag Tools Wiki (<http://www.animaltags.org>), the Chronux spectral analysis toolbox and the Matlab signal processing toolbox, and with customized scripts as described below (‘Calculating heart rate from ECG data’ and ‘Derivation of body movement and orientation metrics from sensor data’).

All animal handling and tagging protocols were approved by Stony Brook University’s Institutional Animal Care and Use Committee (IACUC number 1473497) and by the British Antarctic Survey’s Animal Welfare Ethical Review Process.

#### Calculating heart rate from ECG data

Individual heartbeats were identified in the 600 Hz ECG time series using a signal template detection algorithm implemented in a



Bayesian modeling framework using custom-written code in MATLAB. In brief, the heartbeat signal template was obtained by isolating a mean QRS complex waveform from a high signal-to-noise segment of raw ECG. Prior to applying the detection method to the full ECG data, we first pre-processed the data by applying a low-pass filter with a bandwidth of 0–150 Hz and then used a local detrend on the filtered signal with a moving window length of 1 and step length of 0.1. The resulting data were then differenced using a lag-1 and downsampled by two to remove the correlation introduced into the signal when differencing. These filtered, detrended, differenced data were then used in an iterative backwards and forwards signal detection procedure to identify heartbeats. For a detailed explanation of the Bayesian model used to detect heartbeats and assign peak probabilities, see [Supplementary Materials and Methods](#) ('Bayesian modeling framework for the detection of heart beats from ECG data'). Each heartbeat was associated with a peak probability value ranging from 0 to 1. On average, peak probabilities were high (mean±s.d. of 0.947±0.10) but varied across behaviors. Probabilities were lower during flapping flight (mean±s.d. of 0.88±0.12), likely from interference of the ECG signal due to muscle contractions. Heart rate ( $f_H$ , beats min<sup>-1</sup>) and median peak probability within 30 s windows were calculated throughout the time series. To minimize the inclusion of false heartbeats, we removed those associated with a median peak probability of <0.85, which amounted to 14.1% of the two time series (21.9% and 5.7% for black-browed and grey-headed albatrosses, respectively).

### Estimation of $\dot{V}_{O_2}$ from heart rate

Energetic proxies derived from accelerometer data were compared with  $\dot{V}_{O_2}$ , an indirect measure of metabolic rate, estimated from heart rate. This method has been applied widely to free-ranging animals, but requires  $\dot{V}_{O_2} \approx f_H$  calibrations to be conducted in the laboratory on the same or closely related species (Butler et al., 2004; Green, 2011). We evaluated two methods for estimating  $\dot{V}_{O_2}$  from heart rate in albatrosses: (1) an equation derived from a previous calibration experiment where both  $f_H$  and  $\dot{V}_{O_2}$  were recorded in parallel from black-browed albatrosses exercising on a treadmill (Bevan et al., 1994, 1995); and (2) a cross-taxa avian model in Bishop and Spivey (2013) that estimates  $\dot{V}_{O_2}$  from  $f_H$  for a bird of given mass and heart mass. The formulas are as follows (Bevan et al., 1995):

$$\dot{V}_{O_2} = 0.00466 f_H^{1.61}, \quad (1)$$

where  $\dot{V}_{O_2}$  is in ml min<sup>-1</sup> kg<sup>-1</sup> and  $f_H$  is heart rate in beats min<sup>-1</sup>. Mass-independent  $\dot{V}_{O_2}$  estimates were then multiplied by the mass of each bird (kg) to provide mass-specific  $\dot{V}_{O_2}$  in ml min<sup>-1</sup> (Bishop and Spivey, 2013):

$$\dot{V}_{O_2} = 0.0402 M_b^{0.328 \pm 0.05} M_h^{0.913 \pm 0.045} f_H^{2.065 \pm 0.03}, \quad (2)$$

where  $M_b$  is body mass (kg),  $M_h$  is estimated heart mass (g) and  $f_H$  is heart rate (beats min<sup>-1</sup>). Masses recorded in the field were used to estimate heart mass for each bird using the following allometric relationship (Eqn 3) derived from 18 species of Procellariiformes (Battam, 2010):

$$M_h = 8.51 \pm 1.9 M_b^{0.83 \pm 0.03}. \quad (3)$$

Curves of measured heart rate, and  $\dot{V}_{O_2}$  estimates modeled from heart rate using both equations resulted in similar  $\dot{V}_{O_2}$  estimates (Fig. S1). As the choice of equation had minimal impact on the estimates, we chose the equation from Bevan et al. (1995) as it was derived from direct measurement in black-browed albatrosses. We

hereafter refer to these  $f_H$ -derived estimates of  $\dot{V}_{O_2}$  as simply  $\dot{V}_{O_2}$  in the majority of cases.

### Derivation of body movement and orientation metrics from sensor data

#### Calculation of movement and behavioral metrics

Before analysis, accelerometer and magnetometer data were pre-processed. The 75 Hz triaxial accelerometer and magnetometer signals were reduced to 25 Hz using the '*decdec.m*' function in the TagTools toolbox, a frequency sufficient for identifying major movement behaviors in albatrosses (Conners et al., 2021). Magnetometer and accelerometer sensors were on separate circuit boards, requiring a sensor frame adjustment ( $[X=-Y, Y=-X, Z=Z]$ ) to align the accelerometer sensor axes with the magnetometer and bird frames. All tags sat on the birds with a slight tilt because of the round battery shape, so the tag frame was additionally adjusted using a rotation matrix of Euler angles (using the '*euler2rotmat.m*' and '*rotate\_vecs.m*' functions from the TagTools toolbox). Roll offsets were identified from accelerometer data when birds were resting on land or water, where average heave acceleration was assumed to be ~1 and average sway and surge acceleration to approximate 0. Triaxial magnetometer data were calibrated using a data-driven segmentation method (described in Conners et al., 2021) and large magnetic interferences, likely associated with local magnetic field of other tag components and magnets used to switch tags on and off, were trimmed at the beginning and end of trips. As we were predominately interested in relatively slow heading changes in albatrosses from the magnetometer data, we used a high-pass filter (0.18 Hz cutoff) to remove high-frequency noise in the magnetometer data that was likely introduced by small movements and/or vibrations of the tag and that did not relate to albatross rotations. Following pre-processing, for each axis, static acceleration was derived from total acceleration using a moving-average filter with a 2 s moving window (Shepard et al., 2008). Dynamic acceleration was calculated as the difference between total acceleration and static acceleration. A 25 Hz time series of ODBA was calculated as the sum of the absolute dynamic body acceleration in all three axes (Wilson et al., 2006). VeSBA was calculated similarly, and represents static acceleration in three axes (Wilson et al., 2020). The equations are as follows:

$$\text{ODBA} = |A_{dx}| + |A_{dy}| + |A_{dz}|, \quad (4)$$

$$\text{VeSBA} = (A_{sx}^2 + A_{sy}^2 + A_{sz}^2)^{1/2}, \quad (5)$$

where  $A_d$  is dynamic acceleration and  $A_s$  is static acceleration. We derived ODBA rather than VeDBA (vectorial dynamic body acceleration) as it shows a closer correlation with  $\dot{V}_{O_2}$  (Qasem et al., 2012). Euler angles (pitch, roll and heading) were derived from accelerometer and magnetometer data. Pitch and roll were calculated with the '*a2pr.m*' function from the TagTools toolbox, with pitch constrained to  $\leq 90$  deg (<http://www.animaltags.org>). Each magnetometer axis was rotated according to pitch and roll in a tilt correction procedure to account for postural offsets (Bidder et al., 2015). Heading (with respect to magnetic north) was then calculated as the arctangent of the frame-adjusted  $x$  and  $y$  magnetometer channels using the '*m2h.m*' function from the TagTools toolbox. Pitch, roll and heading were converted from radians to degrees in the range 0–360 deg for analyses.

To quantify movement in heading associated with dynamic soaring, we calculated the angular velocity on the yaw axis (AVEY) as described in Gunner et al. (2020). Given the potential of centripetal acceleration to impact pitch and roll measurements, we

limited our analysis of angular metrics to the yaw axis. Instead of focusing our analysis on instantaneous movements of the albatross along the yaw axis, we focused on changes in yaw on a larger time scale (3 s) in order to capture slower, periodic changes in heading associated with the arcing movement that characterizes dynamic soaring (hereafter termed  $AVeY_{soar}$ ). Because the time window should be less than the time it takes for half a revolution of the animal (Gunner et al., 2020), we selected 3 s for  $AVeY_{soar}$  as the dynamic soaring cycles of albatrosses are typically 8–10 s (Bousquet et al., 2017; Richardson, 2011). Given  $AVeY_{soar}$  was derived from circular heading data (0–360 deg), we corrected for large jumps in heading that were indicative of a 0–360 deg coordinate crossing rather than actual heading changes of the bird. A threshold of 200 deg was selected based on a visual inspection of the  $AVeY_{soar}$  time series and conspicuously large instantaneous jumps observed in the time series. For values >200 deg, we shifted that segment of the  $AVeY_{soar}$  time series using the degree difference between the jump and the last data point before the jump (Fig. S2).

### Flight mode and detection of flaps

To assess whether relationships between  $f_H$ -derived  $\dot{V}_{O_2}$  and movement metrics differed between soaring and flapping flight, we first classified behavior from the accelerometer dataset into three major movement modes using a hidden Markov model (HMM) from Conners et al. (2021) detailed in [Supplementary Materials and Methods](#) ('Classification of accelerometer data into behavior using a hidden Markov model'). The overall accuracy of this model was 91.5%, although this varied across behavioral mode (86.6% for 'flapping flight', 92.6% for 'soaring flight', and 91.7% for 'on-water'). Given the putative high cost of flapping flight, we sought to assess whether the number of flaps provided a useful metric of energy expenditure. While the HMM effectively identified the dominant movement modes ('soaring', 'flapping', 'on-water') in 30 s windows, individual flaps occur on a shorter time scale, and occasionally while birds are soaring or on the water, so we developed an additional method that could be used to derive a metric of the number of flaps ('nFlaps'). A flap was considered a full up and down cycle of the wing that occurs in a single wingbeat. We first ran fast Fourier transforms on the 25 Hz dynamic-heave-acceleration signal in 3 s windows to identify the dominant frequency in that segment. Black-browed and grey-headed albatrosses are known to flap during cruising flight at approximately 2.5–3.1 Hz (Conners et al., 2021; Sakamoto et al., 2013) while flapping during take-off occurs at a lower frequency of ~1.6–2.0 Hz (Sakamoto et al., 2013); therefore, if the dominant frequency of a 3 s segment was between 1.6 and 3.1 Hz, we then identified peaks in that segment using the *findpeaks.m* function in Matlab, and labeled those as individual flaps. A 30 s time series of flapping rate (flaps  $\text{min}^{-1}$ ) was then derived from the vector of flap indices.

### Synchronization of movement metrics and heart rate data

The 25 Hz sensor data and derived movement metrics (ODBA, VeSBA) were binned into 30 s fixed time windows to match the resolution and sync with the times of the processed  $f_H$  data. Within each 30 s window, we calculated the mean and standard deviation of ODBA and VeSBA. We also characterized soaring patterns by quantifying the mean magnitude of the soaring arc (deg) and the frequency (no. arcs  $\text{min}^{-1}$ ). The magnitude of soaring arcs (in the horizontal plane) was identified by finding the local minimum and maximum values (negative and positive peaks) in the  $AVeY_{soar}$  time series that were associated with the amplitude (in horizontal heading

degrees) of the turn of a bird during a dynamic soaring arc (Fig. S2), and we extracted the mean of the absolute values of the peaks in each 30 s window. Arcing rate was calculated as the number of peaks in the 30 s window, converted to arcs  $\text{min}^{-1}$ .

### Statistical analyses

All statistical analyses were implemented in RStudio (v1.2.1335) with the R statistical language (v4.0.3) predominately using general baseR and tidyverse functions and customized scripts, except for some specific packages and functions described in the following methods. The sensor analyses described above resulted in 30 s time series of  $\dot{V}_{O_2}$ , movement metrics, and behavioral state for each deployment.  $f_H$  recovery after intense muscular effort associated with take-off and flapping can be delayed in albatrosses (Weimerskirch et al., 2000). Therefore, following exploratory analyses of these delays, we further binned data into 30 min segments in which behavior and physiology appeared to be in steady state. Movement and physiological metrics were summarized as means and standard deviations; behavioral states were summarized as percentage time in each behavioral state; and flaps were summarized as the number of flaps within each 30 min window (Table 1). When summarizing data into the 30 min datasets, an additional metric of landing rate (landings  $\text{h}^{-1}$ ) was calculated as the number of switches from either of the flight states to the on-water state, as landing rate has been shown to correlate with energy expenditure in foraging albatrosses (Kroeger et al., 2020; Shaffer et al., 2001).

### Behavior-specific energetic costs (objective 1)

We used linear mixed models to evaluate how flight mode influenced mean  $f_H$ -derived  $\dot{V}_{O_2}$  and ODBA values at the 30 min resolution. Species was included as a fixed effect and bird identity as a random effect to account for individual variability (<https://CRAN.R-project.org/package=nlme>). As albatrosses can exhibit a variety of behaviors in a 30 min time frame, we defined the dominant behavioral state as the behavior which took up >90% of the time, and if no behavior was dominant, designated that period as 'mixed' behavior. We chose 90% as the threshold as that was the highest value that led to the retention of enough 30 min segments with flapping flight as the dominant state. We then conducted a *post hoc* test of multiple comparisons of means using Tukey contrasts to compare  $\dot{V}_{O_2}$  and ODBA across the three behavioral states: flapping, soaring and on-water. Unless indicated otherwise, mean values in the results are presented  $\pm$ s.d.

### Prediction of $\dot{V}_{O_2}$ with movement-derived metrics at different temporal scales (objective 2)

To evaluate how movement metrics influenced  $\dot{V}_{O_2}$  at fine time scales, we modeled  $f_H$ -derived  $\dot{V}_{O_2}$  (log<sub>10</sub> transformed) in relation to various movement metrics using a series of linear mixed models (LMMs) in the *lme4* package in R (Bates et al., 2015). The effects of sex and species were included in the initial model configurations but were removed in final models after evaluation using Akaike information criteria for model selection. A total of 3 models were built on 30 min datasets using movement metrics (ODBA, VeSBA and nFlaps). Details of models and the model selection procedure are provided in [Supplementary Materials and Methods](#) ('Linear mixed models'). Given that the accuracy of energetic estimates is likely to increase with increasing time scales (Green, 2011), we evaluated how effectively movement metrics predicted  $\dot{V}_{O_2}$  with increasing timescales (30 min, 12 h, 24 h) in a second set of LMMs ('validation models', Table 2; [Supplementary Materials and](#)

**Table 1. Summary stats of heart rate ( $f_H$ ) and movement metrics for each species overall, and within each behavioral state, calculated from data at a 30 min temporal scale**

Species	$n$	$f_H$ (beats $\text{min}^{-1}$ )	ODBA (g)	VeSBA (g)	No. of flaps	Arc magnitude (deg)	Arc rate (arcs $\text{min}^{-1}$ )
Black-browed	2720	133±15	0.320±0.031	1.099±0.026	176±272	71.7±11.8	15.1±1.30
Flap	41	153±37	0.468±0.052	1.11±0.052	1259±318	NA	NA
Soar	841	126±23	0.367±0.078	1.20±0.071	31.8±36.9	71.7±11.8	15.1±1.30
Water	726	126±27	0.246±0.031	1.00±0.008	19.4±47.6	NA	NA
Grey-headed	2549	143±25	0.345±0.025	1.131±0.305	138±238	72.7±11.1	15.0±1.26
Flap	17	188±50.4	0.459±0.075	1.11±0.034	1404±374	NA	NA
Soar	681	137±29.2	0.382±0.089	1.21±0.066	42.2±62.9	72.7±11.1	15.0±1.26
Water	566	137±35.9	0.255±0.023	1.00±0.017	11.3±34.8	NA	NA

Sample sizes represent the number of observations in each 30 min dataset. The total sample size for each species includes mixed states (i.e. 30 min windows where there was not a dominant behavioral state isolated for behavior-specific analysis).  $f_H$ , heart rate; ODBA, overall dynamic body acceleration; VeSBA, vectorial norm of static body acceleration.

**Methods**, ‘Linear mixed models’). Predicted values were estimated both with and without bird identity as a random effect to evaluate how individual variability affected model predictions.

### Variability in $\dot{V}_{O_2}$ during dynamic soaring (objective 3)

As albatrosses fly predominantly using dynamic soaring, we identified 30 min sections in which soaring flight accounted for >95% of the time (using a higher threshold than in previous analyses to reduce statistical noise). This enabled us to evaluate which metrics best explained variability of  $\dot{V}_{O_2}$  while albatrosses were engaged persistently in this characteristic flight mode where environmental DBA may be highly relevant. Additional LMMs were then built with  $\dot{V}_{O_2}$  as the dependent variable, and explanatory variables as follows: (1) heading-derived metrics associated with rotational movement while dynamic soaring (arc magnitude and arc rate), and (2) accelerometry metrics ODBA and VeSBA. ODBA and VeSBA were evaluated in separate models as they had a correlation >0.60. Mass was included as a fixed effect and bird as a random effect.

## RESULTS

### Time budgets and activity-specific energetic costs (objective 1)

During incubation, black-browed and grey-headed albatrosses were at sea for means of 9.2 and 7.9 days, respectively. The memory capacity of the biologgers was 8.3 days, though the batteries failed after 3.2 and 3.5 days on two devices. During brood-guard, black-browed and grey-headed albatrosses were at sea for means of 2.4 and 3.0 days, respectively; thus brood-guard trips were recorded in full, with three exceptions (when the batteries failed before return). Time-activity budgets were calculated from the 30 s time scale ( $n=167,082$  and  $n=153,327$ , black-browed and grey-headed albatrosses), reported in more detail in a previous study (Connors et al., 2021). In brief, black-browed and grey-headed albatrosses spent most of their trip in flight (62.3±14.7% and 68.1±10.3%,

respectively) and the majority of that flight time was spent dynamic soaring (77.7±10.5% and 83.4±9.6%, respectively), rather than flapping. The average amount of an entire trip spent soaring was 49.2±16.2% and 57.1±12.6%, for black-browed and grey-headed albatrosses, respectively. Albatrosses spent an average of 22.3±10.5% and 16.6±9.6% of flight time in the flapping flight mode, and 13.1±5.6% and 10.9±5.9% of entire foraging trips were spent flapping.

The distributions of  $f_H$  of black-browed and grey-headed albatrosses did not differ significantly (LMM using bird as a random effect; d.f.=24,  $P=0.24$ ), although the tail of the distribution of lighter grey-headed albatrosses was slightly longer, leading to a higher mean  $f_H$  (143±25 versus 133±15 beats  $\text{min}^{-1}$ ) (Fig. S1). Mean  $\dot{V}_{O_2}$  values were 40.7±8.46 ml  $\text{min}^{-1} \text{kg}^{-1}$  and 45.7±15.95 ml  $\text{min}^{-1} \text{kg}^{-1}$  in black-browed and grey-headed albatrosses, respectively. When albatrosses were predominately flapping (>90% of time in each 30 min observation),  $\dot{V}_{O_2}$  was significantly higher [estimated marginal mean (emm)=52.5 ml  $\text{min}^{-1} \text{kg}^{-1}$  (confidence interval, CI=45.2–59.9 ml  $\text{min}^{-1} \text{kg}^{-1}$ ) and emm=57.6 ml  $\text{min}^{-1} \text{kg}^{-1}$  (CI=49.7–65.4 ml  $\text{min}^{-1} \text{kg}^{-1}$ ) in black-browed and grey-headed albatrosses, respectively] than when soaring [emm=38.3 ml  $\text{min}^{-1} \text{kg}^{-1}$  (CI=31.6–45.1 ml  $\text{min}^{-1} \text{kg}^{-1}$ ) and emm=43.4 ml  $\text{min}^{-1} \text{kg}^{-1}$  (CI=36.1–50.6 ml  $\text{min}^{-1} \text{kg}^{-1}$ )] or on the water [emm=37.2 ml  $\text{min}^{-1} \text{kg}^{-1}$  (CI=30.5–44.0 ml  $\text{min}^{-1} \text{kg}^{-1}$ ) and emm=42.3 ml  $\text{min}^{-1} \text{kg}^{-1}$  (CI=35.0–49.6 ml  $\text{min}^{-1} \text{kg}^{-1}$ )] (Fig. 2). Similarly, mean ODBA was significantly higher when birds were predominately flapping; however, unlike the pattern for  $\dot{V}_{O_2}$ , mean ODBA of soaring behavior was significantly higher than for on water behavior (Fig. 2).

### The use of ODBA as a proxy of energy expenditure across flight behaviors (objective 2)

Movement metrics, body mass and number of landings were all significant terms influencing  $\dot{V}_{O_2}$  in models across foraging trips. Sex and species were not significant and were removed from the

**Table 2. Validation model results showing the marginal [ $R^2(m)$ ] and conditional [ $R^2(c)$ ] values and slope from the linear mixed models that evaluated the fit between model-predicted  $\dot{V}_{O_2}$  and  $f_H$ -derived  $\dot{V}_{O_2}$  using mean values calculated at various time scales**

Model used to derive predicted $\dot{V}_{O_2}$	Daily				12 h				30 min			
	$R^2(m)$	$R^2(c)$	Slope	%Diff	$R^2(m)$	$R^2(c)$	Slope	%Diff	$R^2(m)$	$R^2(c)$	Slope	%Diff
ODBA:pSoar+nLandings+mass	0.25	0.78	1.26	7.3, 4.7	0.26	0.72	1.36	6.8, 4.1	0.16	0.51	1.09	5.9, 3.3
VeSBA:pSoar+nLandings+mass	0.18	0.76	1.00	7.3, 4.9	0.20	0.71	1.10	6.8, 4.3	0.17	0.52	1.00	5.7, 3.2
nFlaps+nLandings+mass	0.20	0.77	1.02	7.2, 4.7	0.23	0.73	1.15	6.7, 4.2	0.14	0.52	0.94	5.9, 3.4

Effect size of model error (%Diff) was calculated as the difference between mean model-predicted and  $f_H$ -derived  $\dot{V}_{O_2}$  values as a percentage of mean  $f_H$ -derived  $\dot{V}_{O_2}$  for model predictions. The two %Diff values in each cell represent model error when not accounting for random effect of bird, and when accounting for random effect of bird, respectively.

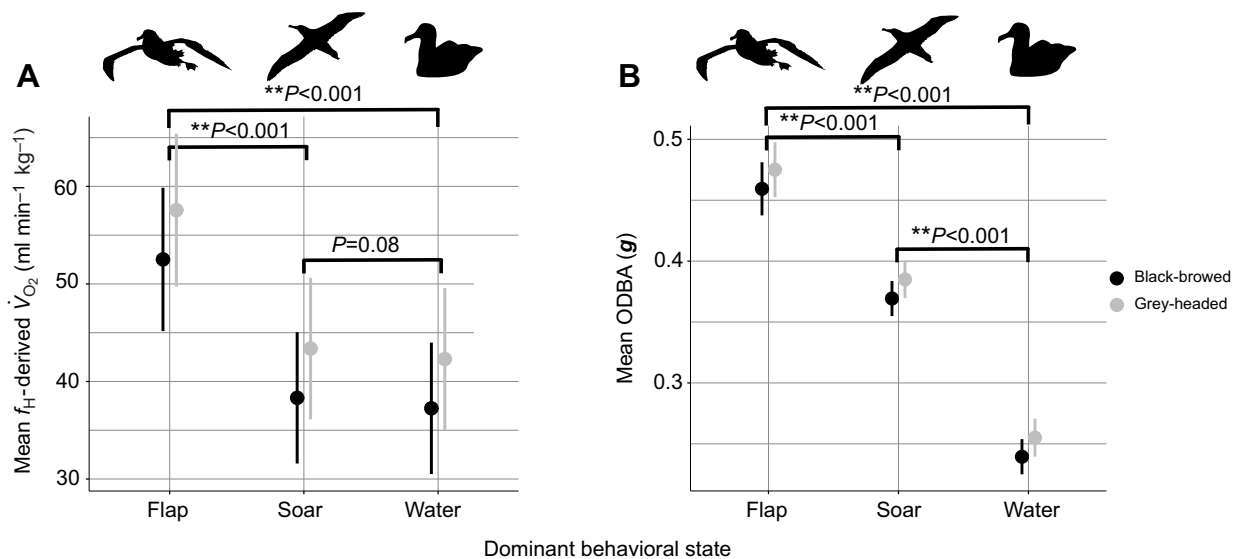


**Fig. 2. Mean  $f_H$ -derived  $\dot{V}_{O_2}$  and overall dynamic body acceleration (ODBA) by dominant behavioral state.** The dominant behavioral state was defined as that behavior which consisted of >90% of the time in each 30 min time frame. If no dominant behavior was present, then it was designated as 'mixed' (not shown in the plots). Data are plotted as estimated marginal means and confidence intervals (CIs) derived from linear mixed models evaluating the response of  $f_H$ -derived  $\dot{V}_{O_2}$  (A) and ODBA (B) to dominant behavioral state with species as a fixed effect and bird as a random effect. *Post hoc* multiple comparison tests using Tukey contrasts evaluated the differences in  $f_H$ -derived  $\dot{V}_{O_2}$  and ODBA across behavioral states (asterisks indicate significance).

final models (Table S1). There was no consistent relationship between ODBA and  $\dot{V}_{O_2}$  across behaviors, indicated by the significant interaction between ODBA and percentage time spent soaring (Table 2, Fig. 3A). When percentage time spent soaring was low (<50%), there was a positive linear relationship between ODBA and  $\dot{V}_{O_2}$ , but the slope decreased with increasing percentage time soaring, becoming negative as time spent soaring approached 100% (Fig. 3A). For example, when time spent soaring was 5% and mean ODBA increased from 0.20 to 0.80 g,  $\dot{V}_{O_2}$  concomitantly increased by 122.9% with a regression slope of 1.34. In contrast, when time spent soaring was 75% and mean ODBA increased from 0.20 to 0.80 g,  $\dot{V}_{O_2}$  only increased by 5.6% with a regression slope of 0.09. Further, when soaring approached 100% of time,  $\dot{V}_{O_2}$  decreased by 19.1% when mean ODBA increased from 0.20 to 0.80 g (slope=-0.35).

### Identifying the best movement metrics and time scales for quantifying energy expenditure in albatrosses across foraging trips (objective 2)

Comparisons of  $\dot{V}_{O_2}$  predicted from movement and behavioral metrics with  $\dot{V}_{O_2}$  derived from  $f_H$  indicated variable performance across models and time scales (Table 2). The relationship between  $\dot{V}_{O_2}$  and VeSBA, and the interaction with percentage time spent soaring, was similar to that between  $\dot{V}_{O_2}$  and ODBA (Fig. 3B). There was a significant positive, linear relationship between  $\dot{V}_{O_2}$  and the number of flaps ('nFlaps') (Fig. 3C). There were also significant positive relationships between  $\dot{V}_{O_2}$  and both body mass and number of landings. Model fits were substantially higher ( $R^2=0.77$  versus 0.20) if bird identity was included as a random effect (Fig. 4). Overall, the energetic cost of flight, and the associated metrics, depended heavily on the proportion of time spent dynamic soaring.

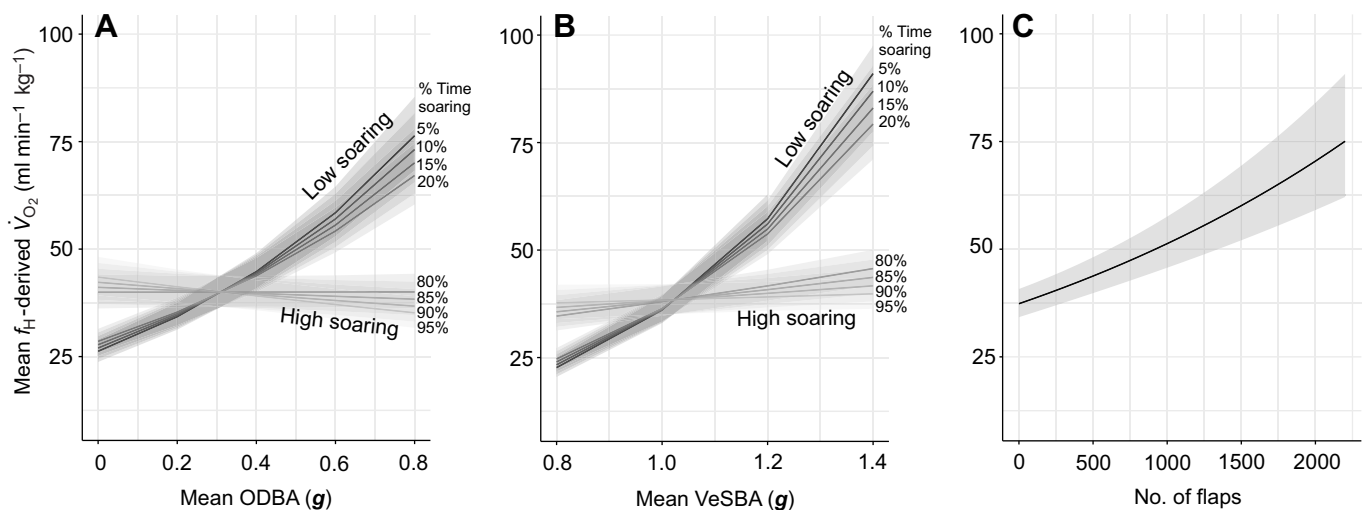


**Fig. 3. Regression results from models evaluating  $f_H$ -derived  $\dot{V}_{O_2}$  across foraging trips (encompassing all behavioral states) as a function of movement metrics.** (A) ODBA, (B) vectorial norm of static body acceleration (VeSBA) and (C) number of flaps. Models a and b included an interaction of each movement metric with the percentage of time spent soaring. Solid lines represent the predicted values of mean  $\dot{V}_{O_2}$  while the shaded area represents the 95% confidence interval.



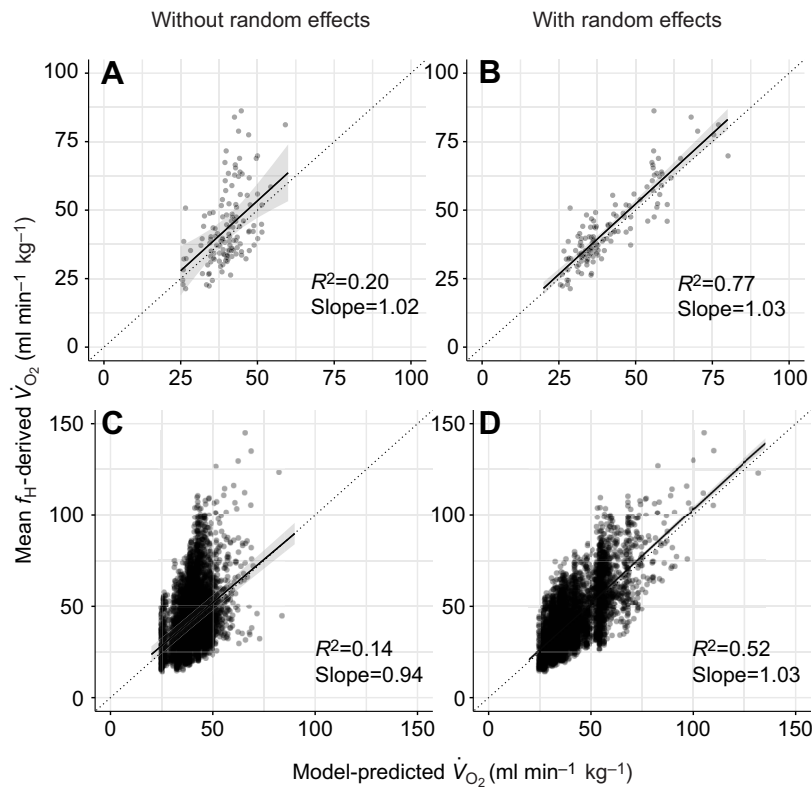


**Fig. 4. An example of the influence of time scale (daily versus 30 min) and random effect of bird on model relationships using the 'nFlaps' model.** Model-predicted  $\dot{V}_{O_2}$  was derived from the model evaluating  $\dot{V}_{O_2} \sim n\text{Flaps} + n\text{Landings} + \text{Mass}$ . (A,B) The relationship between  $\dot{V}_{O_2}$  and the number of flaps is shown at the daily scale (A,B) and at the 30 min scale (C,D). B and D demonstrate the increase in predictive power of the model when the random effect of bird is included in the predictive function, whereas A and C, which represent results that exclude the random effect of bird, show a generalized tendency for movement models to underestimate  $\dot{V}_{O_2}$  at higher  $f_H$ -derived estimates of  $\dot{V}_{O_2}$ . Solid lines represent the predicted values of mean  $\dot{V}_{O_2}$  while the shaded area represents the 95% confidence interval. Circles are all the same color of gray with some level of alpha transparency.

$\dot{V}_{O_2}$  was closely related to ODBA and VeSBA when percentage time spent soaring was low.

The variance explained ( $R^2$ ) was higher for all validation models on a daily time scale than on a 30 min scale [e.g. from marginal  $R^2$ ,  $R^2(m)=0.14$  (30 min) to  $R^2(m)=0.20$  (daily) in the 'nFlaps' model; Fig. 4, Table 2; Fig. S3].  $R^2$  values were highest [ $R^2(m)=0.25$ ] in the model that included ODBA and percentage time soaring models at the daily and 12 h time scales but the slopes deviated most from 1, indicating a consistent underestimation at the higher end value of  $\dot{V}_{O_2}$  derived from  $f_H$ . In general, all models tended to underestimate  $\dot{V}_{O_2}$ , especially at the higher range of values derived from  $f_H$ . However, this effect was small, with a mean percentage difference between model-predicted and  $f_H$ -derived  $\dot{V}_{O_2}$  ranging between 3.1% and 7.3% of mean  $f_H$ -derived  $\dot{V}_{O_2}$  values (Table 2).

### Variability in $\dot{V}_{O_2}$ during dynamic soaring (objective 3)

The distributions of arc magnitudes and arc rates of dynamic soaring albatrosses did not differ significantly between black-browed and grey-headed albatrosses (arc size: LMM,  $n=1479$ , d.f.=26,  $P=0.212$ ; arc rate: LMM,  $n=1479$ , d.f.=24,  $P=0.801$ ). The overall mean value for arc size was  $\sim 72$  deg ( $70.9 \pm 3.7$  deg and  $73.3 \pm 5.1$  deg for black-browed and grey-headed albatrosses, respectively). Arc rate was very consistent, at around 15 arcs  $\text{min}^{-1}$  ( $15.0 \pm 0.60$  and  $14.9 \pm 0.64$  arcs  $\text{min}^{-1}$  for black-browed and grey-headed albatrosses, respectively) (Table 1). Two arcs equate to a full dynamic soaring cycle, so an average arc rate of 15 arcs  $\text{min}^{-1}$  would equate to 8 s per cycle on average. The mean magnitude of the soaring arc explained the most variation in  $\dot{V}_{O_2}$  while birds were predominately soaring, with an increase of  $\sim 4$  ml  $\dot{V}_{O_2} \text{ min}^{-1}$  for every 25 deg increase in arc size ( $P < 0.001$ ,  $R^2=0.56$ ; Fig. 5D). Arc rate did not have a significant effect on variability in  $\dot{V}_{O_2}$  while birds were soaring ( $P=0.21$ ,  $R^2=0.56$ ; Fig. 5C). Mean VeSBA did not have a significant positive effect on  $\dot{V}_{O_2}$  while birds were soaring (VeSBA:  $P=0.61$ ; Fig. 5B). Mean ODBA had a small but significant negative effect on  $\dot{V}_{O_2}$  while

birds were predominately soaring, with higher ODBA associated with lower  $\dot{V}_{O_2}$  ( $P=0.04$ ,  $R^2=0.55$ ; Fig. 5A). These results indicate there may be an energetic cost to soaring associated with body rotation, and that the magnitude of soaring arc can be used as a determinant of energy expenditure while birds are exclusively soaring.

### DISCUSSION

Our findings demonstrate the substantial energy savings made by albatrosses through dynamic soaring. However, the characteristics of this movement are such that acceleration metrics alone are insufficient for comprehensively understanding energy demand associated with their different flight behaviors. Our study therefore adds to growing evidence that alternative proxies to ODBA may improve estimates of energy expenditure in many animals which fly or swim by exploiting environmental energy (Williams et al., 2017; Wilson et al., 2020). ODBA as it is traditionally used, may overestimate energy expenditure when dynamic body accelerations manifest not from contracting muscles but rather from environmental DBA harnessed through body rotations and static postural holds as observed in dynamic soaring seabirds, wave-riding dolphins (Williams et al., 1992) or sharks surfing current updrafts (Papastamatiou et al., 2021). Unlike birds that soar on thermals, albatrosses experience large and rapid gains and losses of acceleration while dynamic soaring (Connors et al., 2021; Fig. S4). These manifest as high values for ODBA but without a concomitant increase in energy expenditure (Figs 2 and 3A). In contrast, there was a much stronger, positive relationship between energy expenditure  $\dot{V}_{O_2}$  and ODBA during periods when birds were mainly engaged in flapping flight (Fig. 3A).

As albatrosses gain kinetic energy from the wind while soaring (Sachs et al., 2012, 2013), the assumption underlying ODBA as a proxy of energy expenditure, which is that rapid gains and losses of acceleration are entirely due to muscular contractions, is violated. Indeed, the largest ODBA values when albatrosses were



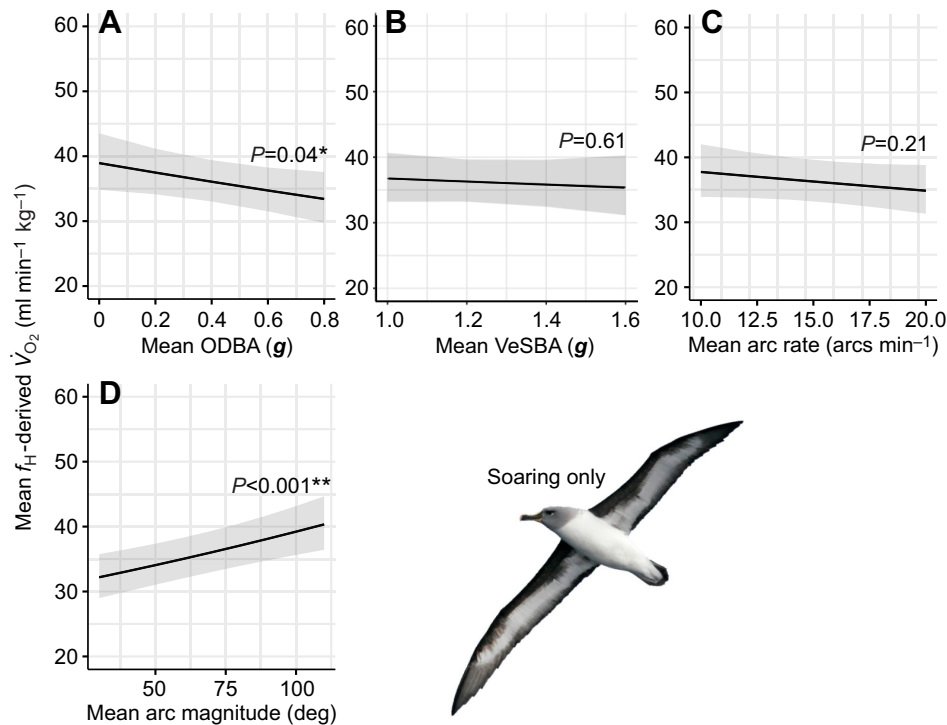


**Fig. 5. Results from linear mixed models evaluating the effect of various movement metrics (top) and soaring-specific metrics (bottom) on  $f_H$ -derived  $\dot{V}_{O_2}$  while birds were predominately soaring.** Arc magnitude (D) had the strongest effect on  $f_H$ -derived  $\dot{V}_{O_2}$ , with increasing arc size relating to increasing  $f_H$ -derived  $\dot{V}_{O_2}$ . ODBA (A) showed a marginally significant, but negative, effect on  $f_H$ -derived  $\dot{V}_{O_2}$  while birds were soaring, with larger ODBA values relating to lower  $f_H$ -derived  $\dot{V}_{O_2}$ . Sample sizes for 30 min periods of soaring were: black-browed albatrosses 664 (14 individuals) and grey-headed albatrosses 838 (12 individuals).

predominately soaring were associated with slightly lower energy expenditure (Fig. 3A), suggesting that birds which soared with greater acceleration actually incurred lower energetic costs. These higher ODBA values are likely associated with stronger winds as albatrosses fly faster in stronger winds and stronger winds sustain longer bouts of continuous soaring relative to lighter winds, which can require intermittent flapping to remain aloft (Schoombie et al., 2023a). An additional yet unexplored explanation is that the shoulder-locking mechanism in albatrosses may work more effectively under stronger lift forces experienced in higher winds, which would lessen the extent of isometric contractions required for the postural holds maintained during soaring flight. Thus, ODBA alone is a poor predictor of energy expenditure in albatrosses. Nevertheless, when accounting for time spent soaring, ODBA and VeSBA can serve as useful metrics to predict energy expenditure across both short and long time scales (30 min to daily), as can the number of flaps (Table 2). Given the opposing relationships with  $\dot{V}_{O_2}$  and ODBA between flapping and soaring, we anticipated that models would more accurately predict  $\dot{V}_{O_2}$  in birds that spent more of their trip in flapping flight. Indeed, the absolute mean error for each bird increased with the time spent soaring in all models; however, this effect was marginally non-significant (Fig. S5). This highlights the importance of accurately quantifying flapping in energetic studies, particularly over longer time scales, and further underscores the efficiency of dynamic soaring relative to flapping flight in albatrosses. Our results suggest that the number of flaps (as well as ODBA and VeSBA) can be an effective metric to understand broad-scale energetics even in birds that predominately use dynamic soaring as long as these metrics are evaluated with behavior. This is particularly promising as these metrics can be easily measured using accelerometry, and long deployments of accelerometers are now possible (Brown et al., 2022), although assessing time spent soaring, as in the present study, requires the additional and more labor-intensive step of classifying behavior (Conners et al., 2021). All metrics were poor predictors of  $\dot{V}_{O_2}$  at the near-instantaneous resolution of our fundamental dataset (30 s), likely due to the

observed lag in  $f_H$  response relative to the time involved in switching behaviors. Conversely, predictive power of models improved with increasing time scales, a probable consequence of integrating both the lagged  $f_H$  response to behavioral switching and the influence of external factors beyond movement that, too, influence physiology. Further work can use these results and their interpretation to inform targeted decision making on time scales and metrics to use in energetic studies on albatrosses and other similar species.

All models predicted estimated  $\dot{V}_{O_2}$  accurately when individual identity was included as a random effect ( $R^2$  values  $>0.70$ ), but underestimated  $\dot{V}_{O_2}$  (based on  $f_H$ ) when individual effects were not taken into consideration (Table 2, Fig. 4). This may be an artifact of substantial intra-specific differences in the relationship between  $f_H$  and  $\dot{V}_{O_2}$ , which was also the case for albatrosses exercising in a respirometer (Bevan et al., 1994, 1995; see also Green, 2011). As the equation we used to derive  $\dot{V}_{O_2}$  from  $f_H$  (Eqn 1) was obtained from animals in a previous calibration study, there is inevitably some inherent error in  $\dot{V}_{O_2}$  estimates due to individual variability. Factors driving individual differences in the relationships between  $\dot{V}_{O_2}$  and movement metrics are challenging to identify (Crossin et al., 2014). However, they may be intrinsic and reflect long-term differences in fitness (Grémillet et al., 2018). Moreover, the individual albatrosses in our study would have encountered a wide range of external conditions, particularly in terms of wind, temperature or psychosocial stimuli, and associated physiological responses would affect  $f_H$  independent of movement. Regardless, we found robust relationships between the various movement metrics and  $\dot{V}_{O_2}$  estimated from  $f_H$ , and the mean differences between model-predicted  $\dot{V}_{O_2}$  (without individual effects) and  $\dot{V}_{O_2}$  estimated from  $f_H$  were small (3–7%). This indicates a lack of systematic bias, and that the models presented here can be applied for examining broad-scale energetics of albatrosses beyond the birds in our study.

Only recently have accelerometer- and magnetometer-derived metrics of rotation (e.g. absolute angular velocity, ‘AAV’: Gunner et al., 2021; rate of change of rotational movement, ‘RocRM’: Hopkins et al., 2021) been linked to animal behavior

(Gunner et al., 2021) and energy expenditure (Hopkins et al., 2021). Gyroscopes have long been the standard for quantifying instantaneous rotational metrics; however, these sensors are highly sensitive to environmental conditions (e.g. temperature), consume large amounts of power relative to accelerometers and magnetometers, and require large batteries and/or short deployment durations and thus have not been widely applied to energetic studies of free-ranging animals. Magnetometers, in contrast, are inexpensive and power efficient, making them a more accessible tool for understanding energetics and behavior in free-ranging wildlife populations, particularly those that use movement modalities than involve triaxial rotation. While we could not reliably quantify AAV in our dataset because of potential error introduced to pitch and roll measurements when birds were banking sharply, as is common during dynamic soaring, the association between energy expenditure and the arcing magnitude of soaring birds suggests costs of rotation play a role. Angular velocity on the roll axis ('AvER': Gunner et al., 2020) in particular has the potential to track energy expenditure in soaring albatrosses given the continuous sharp banking that occurs on the roll axis during dynamic soaring flight. Future work on albatross flight energetics should explore methodologies and developments in tag technology (e.g. power-efficient gyroscopes, miniaturized cameras, pitch/roll correction factors) to obtain this metric in a reliable manner (e.g. Schoombie et al., 2023b).

The positive relationship between arcing magnitude and energy expenditure may reflect energetic costs from both rotation and additional muscular movement to avoid flight instabilities when maintaining a steep bank angle. Understanding the energetic costs of soaring is fundamental given it is the predominant flight mode (up to 75% of foraging trips by the tracked birds) of albatrosses. Albatrosses and other seabirds that use dynamic soaring rotate their bodies repeatedly over sustained periods to travel long distances, and so energetic costs inevitably accumulate. For example, an albatross soaring for 75% of its trip at an average rate of 15 arcs  $\text{min}^{-1}$  would make  $\sim 21,600$  rotations per day. Thus, the energetic costs of these rotational movements, even if small relative to power movements such as flapping, are critical for gaining a comprehensive understanding of the costs of locomotion. It is not just albatrosses for which it is important to quantify the energetic costs of rotational movements but also other birds that use dynamic soaring, and indeed any swimming or flying animals that move freely through volumetric fluid-based environments (Burt de Perera and Holbrook, 2012).

The importance of understanding energetic costs associated with rotational movements and postural control during dynamic soaring becomes clear when considering that oxygen consumption associated with the largest arc sizes (90 deg) was estimated at 39  $\text{ml min}^{-1} \text{kg}^{-1}$  (emm), representing a 15% increase (by 6  $\text{ml min}^{-1} \text{kg}^{-1}$ ) compared with an arc size of 40 deg. If 1  $\text{ml O}_2$  has an energy equivalence of 20.112 J for an albatross (Bevan et al., 1995), then over the course of an hour, birds soaring in large arcs (90 deg) will use an additional  $\sim 7240 \text{ J kg}^{-1}$ . Thus, for a bird of 3.5 kg over a typical 3 day trip involving 53% of time spent dynamic soaring, that would amount to an increase in energy intake of  $\sim 1135 \text{ kJ}$ . That would be equivalent to an additional 284 g of Antarctic krill, *Euphausia superba*, one of the most common items in the diet of both black-browed and grey-headed albatrosses (Mills et al., 2020), with a calorific content of 4  $\text{kJ g}^{-1}$  wet mass (Clarke and Prince, 1980). However, it is also important to consider potential trade-offs as there may be a benefit in terms of prey encounter rates, as birds with larger arcs also showed faster ground speeds, and for opportunistic predators such as albatrosses, covering more ocean

may equate to increased foraging opportunities (Weimerskirch et al., 2012).

It is important to note that pitch and roll values while the birds were experiencing large banking angles may have been impacted by centripetal acceleration and therefore may have introduced some error in the calculation of some heading values; however, we were primarily concerned with the magnitude of changes in heading to describe soaring characteristics (e.g. arc size and arcing rate derived from  $\text{AVeY}_{\text{soar}}$ ) rather than the true cardinal direction of the heading as needed for analyses such as dead reckoning, etc. Further, our distributions of soaring characteristics (arc size and arc rate) derived from the heading and  $\text{AVeY}_{\text{soar}}$  time series were well within the range of what we anticipated based on previously published data on soaring characteristics of albatrosses (e.g. Bousquet et al., 2017; Schoombie et al., 2023a).

There is potential for animal-borne tagging devices to influence behavior or have negative impacts (Gillies et al., 2020; Chivers et al., 2016; Bodey et al., 2018). To minimize the inclusion of data where behavior may have been altered by handling during tag deployments or by the bird acclimating to the device, we trimmed the beginning of the datasets by 2 h. An initial inspection of data showed elevated  $f_H$  for short periods of time (typically well under 30 min) after the initial tagging procedure, after which  $f_H$  slowed to within a normal range. Breeding success of birds fitted with devices was higher than average for the respective colony (46.2% versus 26.8% in black-browed albatrosses, and 35.7% versus 31.8% in grey-headed albatrosses; British Antarctic Survey, unpublished data). This is likely because we did not deploy devices on birds until, at minimum, the end of the second incubation stint, avoiding the initial period of higher failure post-laying. Additionally, the protocol for bird selection included deploying on more experienced breeders which typically have higher success than new recruits (Froy et al., 2017). As such, there was no evidence that the deployments had deleterious effects.

By using high-resolution sensors such as accelerometers and magnetometers to describe dynamic movement (ODBA), postural movement (VeSBA) and fine-scale flight behavior (number of flaps, soaring arc magnitude and rate), we illustrated a link between albatross behavior and energetics at a scale and extent previously unattainable. Providing this link between fine-scale movement and energetics will promote further understanding of the mechanisms driving the energetics of larger-scale behaviors, such as the differential costs of commuting flight, area-restricted search flight (i.e. flight sinuosity) and resting. This link, too, will better equip us to understand the mechanisms driving costs related to varying environmental conditions, such as wind patterns. For example, optimal wind conditions for albatrosses may occur in an envelope between low winds (below which would induce flapping flight) and high winds (which may incur additional costs if high winds require larger soaring arc magnitudes). Wind is particularly important to maintain efficient flight in albatrosses given their dominant flight mode of dynamic soaring, which relies on a sufficiently strong wind gradient. Providing links between behavior, energetics and wind will facilitate the understanding of not just which wind patterns are most optimal energetically speaking but why. This mechanistic understanding is timely as global winds change in response to a changing climate, particularly at higher latitudes where most albatrosses spend their lives.

## Conclusion

We found that  $\dot{V}_{\text{O}_2}$  and dynamic acceleration were decoupled during dynamic soaring in albatrosses, highlighting the limitations of

ODBA as a proxy for energy expenditure in animals that extract environmental energy for movement. Alternative metrics derived from both magnetometers and accelerometers, such as magnitude of soaring arcs, better described the energetics of dynamic soaring, the dominant flight mode of albatrosses. Nonetheless, when modeled as an interaction with percentage time soaring, ODBA accurately predicted  $\dot{V}_{O_2}$  in albatrosses as did the number of flaps, particularly at longer time scales. While the cost of flapping relative to soaring was high, soaring metrics indicated a measurable cost to dynamic soaring likely driven by the cost of rotation. While rotation costs were small, we demonstrated how they can accumulate over time in a non-negligible way for animals whose dominant movement modalities involve continuous rotations. By exploring energetics specific to dynamic soaring, one of the most efficient flight modes in birds, we demonstrate the promise of rotational metrics for developing a more comprehensive understanding of animal energetics.

#### Acknowledgements

We thank Rosamund Hall, Mark Whiffin, Freya Blockley and Alexandra Dodds for assisting with fieldwork at Bird Island, and we thank the Bird Island Research Station, Bird Island, South Georgia, for facility support. This work represents a contribution to the Ecosystems component of the British Antarctic Survey Polar Science for Planet Earth Programme, funded by the Natural Environment Research Council.

#### Competing interests

The authors declare no competing or financial interests.

#### Author contributions

Conceptualization: M.G.C., J.A.G., R.A.P., L.H.T.; Methodology: M.G.C., J.A.G., R.A.P., C.C., P.M.D., A.L.V., L.H.T.; Validation: M.G.C., R.A.O., E.H.; Formal analysis: M.G.C.; Investigation: M.G.C., L.H.T.; Resources: P.M.D., A.L.V., L.H.T.; Data curation: M.G.C., E.H., R.A.O.; Writing - original draft: M.G.C., J.A.G., L.H.T.; Writing - review & editing: M.G.C., J.A.G., R.A.P., R.A.O., C.C., P.M.D., E.H., A.L.V., L.H.T.; Supervision: R.A.P., L.H.T.; Project administration: M.G.C., R.A.P., L.H.T.; Funding acquisition: R.A.P., L.H.T.

#### Funding

Funding was provided by a National Science Foundation CAREER award to L.H.T. (award no. 79804).

#### Data availability

Data including heart rate, behavioral state and movement metrics at the 30 min time scale are available from GitHub: [https://github.com/melindaconners/albatrossenergetics/blob/main/Connors\\_et\\_al\\_JEB2024.csv](https://github.com/melindaconners/albatrossenergetics/blob/main/Connors_et_al_JEB2024.csv)

#### References

- Adams, N. J., Brown, C. R. and Nagy, K. A. (1986). Energy expenditure of free-ranging wandering albatrosses *Diomedea exulans*. *Physiol. Zool.* **59**, 583-591. doi:10.1086/physzool.59.6.30158606
- Bates, D., Mächler, M., Bolker, B. and Walker, S. (2015). Fitting linear mixed-effects models using lme4. *J. Stat. Softw.* **67**, 1-48. doi:10.18637/jss.v067.i01
- Battam, H. (2010). Energetics and morphometrics of non-breeding albatrosses. PhD thesis, School of Biological Sciences, University of Wollongong. <https://ro.uow.edu.au/theses/3245>.
- Bevan, R. M., Woakes, A. J., Butler, P. J. and Boyd, I. L. (1994). The use of heart rate to estimate oxygen consumption to estimate oxygen consumption of free-ranging black-browed albatross *Diomedea melanophrys*. *J. Exp. Biol.* **193**, 119-137. doi:10.1242/jeb.193.1.119
- Bevan, R. M., Butler, P. J., Woakes, A. J. and Prince, E. A. (1995). The energy expenditure of free-ranging black-browed albatrosses. *Philos. Trans. R. Soc. B: Biol. Sci.* **350**, 119-131. doi:10.1098/rstb.1995.0146
- Bidder, O. R., Walker, J. S., Jones, M. W., Holton, M. D., Urge, P., Scantlebury, D. M., Marks, N. J., Magowan, E. A., Maguire, I. E. and Wilson, R. P. (2015). Step by step: reconstruction of terrestrial animal movement paths by dead-reckoning. *Mov. Ecol.* **3**, 23. doi:10.1186/s40462-015-0055-4
- Bishop, C. M. and Spivey, R. J. (2013). Integration of exercise response and allometric scaling in endotherms. *J. Theor. Biol.* **323**, 11-19. doi:10.1016/j.jtbi.2013.01.002
- Bodey, T. W., Cleasby, I. R., Bell, F., Parr, N., Schultz, A., Votier, S. C. and Bearhop, S. (2018). A phylogenetically controlled meta-analysis of biologging device effects on birds: deleterious effects and a call for more standardized reporting of study data. *Methods Ecol. Evol.* **9**, 946-955. doi:10.1111/2041-210X.12934
- Bookmythe, I., Detto, T. and Backwell, P. R. Y. (2008). Female fiddler crabs settle for less: the travel costs of mate choice. *Anim. Behav.* **76**, 1775-1781. doi:10.1016/j.anbehav.2008.07.022
- Bousquet, G. D., Triantafyllou, M. S. and Slotine, J. J. E. (2017). Optimal dynamic soaring consists of successive shallow arcs. *J. R. Soc. Interface* **14**, 20170496. doi:10.1098/rsif.2017.0496
- Brown, J. M., Bouten, W., Camphuysen, K. C. J., Nolet, B. A. and Shamoun-Baranes, J. (2022). Acceleration as a proxy for energy expenditure in a facultative-soaring bird: comparing dynamic body acceleration and time-energy budgets to heart rate. *Funct. Ecol.* **36**, 1627-1638.
- Burt De Perera, T. and Holbrook, R. I. (2012). Three-dimensional spatial representation in freely swimming fish. *Cogn. Process* **13**, 107-111. doi:10.1007/s10339-012-0473-9
- Butler, P. J., Green, J. A., Boyd, I. L. and Speakman, J. R. (2004). Measuring metabolic rate in the field: the pros and cons of the doubly labelled water and heart rate methods. *Funct. Ecol.* **18**, 168-183. doi:10.1111/j.0269-8463.2004.00821.x
- Cavagna, G. A., Saibene, F. P. and Margaria, R. (1963). External work in walking. *J. Appl. Physiol.* **18**, 1-9. doi:10.1152/jappl.1963.18.1.1
- Chapman, J. W., Klaassen, R. H. G., Drake, V. A., Fossette, S., Hays, G. C., Metcalfe, J. D., Reynolds, A. M., Reynolds, D. R. and Alerstam, T. (2011). Animal orientation strategies for movement in flows. *Curr. Biol.* **21**, R861-R870. doi:10.1016/j.cub.2011.08.014
- Chivers, L. S., Hatch, S. A. and Elliott, K. H. (2016). Accelerometry reveals an impact of short-term tagging on seabird activity budgets. *Condor: Ornithol. Appl.* **118**, 159-168. doi:10.1650/CONDOR-15-66.1
- Clarke, A. and Prince, P. A. (1980). Chemical composition and calorific value of food fed to mollymauk chicks *Diomedea melanophrys* and *D. chrysostoma* at Bird Island, South Georgia. *Ibis* **122**, 488-494. doi:10.1111/j.1474-919X.1980.tb00903.x
- Connors, M. G., Michelot, T., Heywood, E. I., Orben, R. A., Phillips, R. A., Vyssotski, A. L., Shaffer, S. A. and Thorne, L. H. (2021). Hidden Markov models identify major movement modes in accelerometer and magnetometer data from four albatross species. *Mov. Ecol.* **9**, 7. doi:10.1186/s40462-021-00243-z
- Costa, D. P. and Prince, P. A. (1987). Foraging energetics of gray-headed albatrosses *Diomedea chrysostoma* at Bird Island, South Georgia [South Atlantic Ocean]. *Ibis* **129**, 149-158. doi:10.1111/j.1474-919X.1987.tb03196.x
- Crossin, G. T., Cooke, S. J., Goldbogen, J. A. and Phillips, R. A. (2014). Tracking fitness in marine vertebrates: a review of current knowledge and opportunities for future research. *Mar. Ecol. Prog. Ser.* **496**, 1-17. doi:10.3354/meps10691
- Duriez, O., Kato, A., Tromp, C., Dell'omo, G., Vyssotski, A. L., Sarrazin, F. and Ropert-Coudert, Y. (2014). How cheap is soaring flight in raptors? A preliminary investigation in freely-flying vultures. *PLoS One* **9**, e84887. doi:10.1371/journal.pone.0084887
- Froy, H., Lewis, S., Nussey, D. H., Wood, A. G. and Phillips, R. A. (2017). Contrasting drivers of reproductive ageing in albatrosses. *J. Anim. Ecol.* **86**, 1022. doi:10.1111/1365-2656.12712
- Gallagher, A. J., Creel, S., Wilson, R. P. and Cooke, S. J. (2017). Energy landscapes and the landscape of fear. *Trends Ecol. Evol.* **32**, 88-96. doi:10.1016/j.tree.2016.10.010
- Gillies, N., Fayet, A. L., Padget, O., Syposz, M., Wynn, J., Bond, S., Evry, J., Kirk, H., Shoji, A., Dean, B. et al. (2020). Short-term behavioural impact contrasts with long-term fitness consequences of biologging in a long-lived seabird. *Sci. Rep.* **10**, 15056. doi:10.1038/s41598-020-72199-w
- Gleiss, A. C., Gruber, S. H. and Wilson, R. P. (2009). Multi-channel data-logging: towards determination of behaviour and metabolic rate in free-swimming sharks. In *Tagging and Tracking of Marine Animals with Electronic Devices*, pp.211-228. Springer.
- Gleiss, A. C., Wilson, R. P. and Shepard, E. L. C. (2011). Making overall dynamic body acceleration work: on the theory of acceleration as a proxy for energy expenditure. *Methods Ecol. Evol.* **2**, 23-33. doi:10.1111/j.2041-210X.2010.00057.x
- Gómez Laich, A., Wilson, R. P., Gleiss, A. C., Shepard, E. L. C. and Quintana, F. (2011). Use of overall dynamic body acceleration for estimating energy expenditure in cormorants. Does locomotion in different media affect relationships? *J. Exp. Mar. Biol. Ecol.* **399**, 151-155. doi:10.1016/j.jembe.2011.01.008
- Green, J. A. (2011). The heart rate method for estimating metabolic rate: review and recommendations. *Comp. Biochem. Physiol. A* **158**, 287-304. doi:10.1016/j.cbpa.2010.09.011
- Green, J. A., Halsey, L. G., Wilson, R. P. and Frappell, P. B. (2009). Estimating energy expenditure of animals using the accelerometry technique: activity, inactivity and comparison with the heart-rate technique. *J. Exp. Biol.* **212**, 745-746. doi:10.1242/jeb.030049
- Grémillet, D., Lescoeur, A., Ballard, G., Dugger, K. M., Massaro, M., Porzig, E. L. and Ainley, D. G. (2018). Energetic fitness: field metabolic rates assessed via 3D accelerometry complement conventional fitness metrics. *Funct. Ecol.* **32**, 1203-1213. doi:10.1111/1365-2435.13074
- Gunner, R. M., Wilson, R. P., Holton, M. D., Scott, R., Hopkins, P. and Duarte, C. M. (2020). A new direction for differentiating animal activity based on measuring angular velocity about the yaw axis. *Ecol. Evol.* **10**, 7872-7886. doi:10.1002/ece3.6515



- Gunner, R., Wilson, R., Holton, M., Scott, R., Arkwright, A., Fahlman, A., Ulrich, M., Hopkins, P., Duarte, C. and Eizaguirre, C. (2021). Activity of loggerhead turtles during the U-shaped dive: new insights using angular velocity metrics. *Endang. Species Res.* **45**, 1-12. doi:10.3354/esr01125
- Halsey, L. G., Shepard, E. L. C., Hulston, C. J., Venables, M. C., White, C. R., Jeukendrup, A. E. and Wilson, R. P. (2008). Acceleration versus heart rate for estimating energy expenditure and speed during locomotion in animals: tests with an easy model species, *Homo sapiens*. *Zoology* **111**, 231-241. doi:10.1016/j.zool.2007.07.011
- Halsey, L., Shepard, E. L. C., Quintana, F., Gomez Laich, A., Green, J. A. and Wilson, R. P. (2009). The relationship between oxygen consumption and body acceleration in a range of species. *Comp. Biochem. Physiol. A: Mol. Integr. Physiol.* **15**, 197-202. doi:10.1016/j.cbpa.2008.09.021
- Halsey, L. G., Shepard, E. L. C. and Wilson, R. P. (2011). Assessing the development and application of the accelerometry technique for estimating energy expenditure. *Comp. Biochem. Physiol. A: Mol. Integr. Physiol.* **158**, 305-314. doi:10.1016/j.cbpa.2010.09.002
- Hopkins, L. W., Gerald, N. R., Pope, E. C., Holton, M. D., Lurgi, M., Duarte, C. M. and Wilson, R. P. (2021). Testing angular velocity as a new metric for metabolic demands of slow-moving marine fauna: a case study with giant spider conchs *Lambis truncata*. *Anim. Biotelemetry* **9**, 1-13. doi:10.1186/s40317-021-00255-x
- Jeannin-Du-Doit, T., Trites, A. W., Arnold, J. P. Y., Speakman, J. R. and Guinet, C. (2016). Flipper strokes can predict energy expenditure and locomotion costs in free-ranging northern and Antarctic fur seals. *Sci. Rep.* **6**, 33912. doi:10.1038/srep33912
- Kroeger, C. E., Crocker, D. E., Orben, R. A., Thompson, D. R., Torres, L. G., Sagar, P. M., Sztukowski, L. A., Andriese, T., Costa, D. P. and Shaffer, S. A. (2020). Similar foraging energetics of two sympatric albatrosses despite contrasting life histories and wind-mediated foraging strategies. *J. Exp. Biol.* **223**, jeb228585. doi:10.1242/jeb.228585
- Martin Lopez, L. M., Aguilar De Soto, N., Madsen, P. T. and Johnson, M. (2022). Overall dynamic body acceleration measures activity differently on large versus small aquatic animals. *Methods Ecol. Evol.* **13**, 447-458. doi:10.1111/2041-210X.13751
- Meyers, R. A. and Stakebake, E. F. (2005). Anatomy and histochemistry of spread-wing posture in birds. 3. Immunohistochemistry of flight muscles and the "shoulder lock" in albatrosses. *J. Morphol.* **263**, 12-29. doi:10.1002/jmor.10284
- Mills, W. F., Xavier, J. C., Bearhop, S., Chereh, Y., Votier, S. C., Waluda, C. M. and Phillips, R. A. (2020). Long-term trends in albatross diets in relation to prey availability and breeding success. *Mar. Biol.* **167**, 29. doi:10.1007/s00227-019-3630-1
- Milner-Gulland, E. J., Fryxell, J. M. and Sinclair, A. R. E. (2011). *Animal Migration: A Synthesis*. OUP Oxford.
- Nathan, R., Spiegel, O., Fortmann-Roe, S., Harel, R., Wikelski, M. and Getz, W. M. (2012). Using tri-axial acceleration data to identify behavioral modes of free-ranging animals: general concepts and tools illustrated for griffon vultures. *J. Exp. Biol.* **215**, 986-996. doi:10.1242/jeb.058602
- Papastamatiou, Y. P., Iosilevskii, G., Di Santo, V., Huvneers, C., Hattab, T., Planes, S., Ballesta, L. and Mourier, J. (2021). Sharks surf the slope: current updrafts reduce energy expenditure for aggregating marine predators. *J. Anim. Ecol.* **90**, 2302-2314. doi:10.1111/1365-2656.13536
- Pennycuik, C. J. (1982). The flight of petrels and albatrosses (Procellariiformes), observed in South Georgia and its vicinity. *Philos. Trans. R. Soc. Lond. B Biol. Sci.* **300**, 75-106. doi:10.1098/rstb.1982.0158
- Pennycuik, C. J. (2008). *Modelling the Flying Bird*. Elsevier.
- Phillips, R. A., Xavier, J. C. and Croxall, J. P. (2003). Effects of satellite transmitters on albatrosses and petrels. *Auk* **120**, 1082-1090. doi:10.1642/0004-8038(2003)120[1082:EOSTOAJ]2.0.CO;2
- Phillips, R. A., Silk, J. R. D., Phalan, B., Catry, P. and Croxall, J. P. (2004). Seasonal sexual segregation in two *Thalassarche* albatross species: competitive exclusion, reproductive role specialization or foraging niche divergence? *Proc. Biol. Sci. R. Soc.* **271**, 1283-1291. doi:10.1098/rspb.2004.2718
- Qasem, L., Cardew, A., Wilson, A., Griffiths, I., Halsey, L. G., Shepard, E. L. C., Gleiss, A. C. and Wilson, R. P. (2012). Tri-axial dynamic acceleration as a proxy for animal energy expenditure; should we be summing values or calculating the vector? *PLoS One* **7**, e31187. doi:10.1371/journal.pone.0031187
- Richardson, P. L. (2011). How do albatrosses fly around the world without flapping their wings? *Prog. Oceanogr.* **88**, 46-58. doi:10.1016/j.pocean.2010.08.001
- Richardson, P. L., Wakefield, E. D. and Phillips, R. A. (2018). Flight speed and performance of the wandering albatross with respect to wind. *Mov. Ecol.* **6**, 3. doi:10.1186/s40462-018-0121-9
- Saadat, M., Fish, F. E., Domei, A. G., Di Santo, V., Lauder, G. V. and Haj-Hariri, H. (2017). On the rules for aquatic locomotion. *Phys. Rev. Fluids* **2**, 83102. doi:10.1103/PhysRevFluids.2.083102
- Sakamoto, K. Q., Takahashi, A., Iwata, T., Yamamoto, T., Yamamoto, M. and Trathan, P. N. (2013). Heart rate and estimated energy expenditure of flapping and gliding in black-browed albatrosses. *J. Exp. Biol.* **216**, 3175-3182. doi:10.1242/jeb.079905
- Sachs, G., Traugott, J., Nesterova, A. P., Dell'omo, G., Kümmeth, F., Heidrich, W., Vyssotski, A. L. and Bonadonna, F. (2012). Flying at no mechanical energy cost: disclosing the secret of wandering albatrosses. *PLoS One* **7**, e41449. doi:10.1371/journal.pone.0041449
- Sachs, G., Traugott, J., Nesterova, A. P. and Bonadonna, F. (2013). Experimental verification of dynamic soaring in albatrosses. *J. Exp. Biol.* **216**, 4222-4232. doi:10.1242/jeb.085209
- Schoombie, S., Wilson, R. and Ryan, P. (2023a). Wind driven effects on the fine-scale flight behaviour of dynamic soaring wandering albatrosses. *Mar. Ecol. Prog. Ser.* **723**, 119-134. doi:10.3354/meps14265
- Schoombie, S., Wilson, R. P. and Ryan, P. G. (2023b). A novel approach to seabird posture estimation: finding roll and yaw angles of dynamic soaring albatrosses using tri-axial magnetometers. *R. Soc. Open sci.* **10**, 231363. doi:10.1098/rsos.231363
- Shaffer, S. A. (2011). A review of seabird energetics using the doubly labeled water method. *Comp. Biochem. Physiol. A Mol. Integr. Physiol.* **158**, 315-322. doi:10.1016/j.cbpa.2010.07.012
- Shaffer, S. A., Costa, D. P. and Weimerskirch, H. (2001). Behavioural factors affecting foraging effort of breeding wandering albatrosses. *J. Anim. Ecol.* **70**, 864-874. doi:10.1046/j.0021-8790.2001.00548.x
- Shepard, E., Wilson, R., Quintana, F., Gómez Laich, A., Liebsch, N., Albareda, D., Halsey, L., Gleiss, A., Morgan, D., Myers, A. et al. (2008). Identification of animal movement patterns using tri-axial accelerometry. *Endang. Species Res.* **10**, 47-60. doi:10.3354/esr00084
- Usherwood, J. R., Stavrou, M., Lowe, J. C., Roskilly, K. and Wilson, A. M. (2011). Flying in a flock comes at a cost in pigeons. *Nature* **474**, 494-497. doi:10.1038/nature10164
- Wakefield, E. D., Phillips, R. A., Matthiopoulos, J., Fukuda, A., Higuchi, H., Marshall, G. J. and Trathan, P. N. (2009). Wind field and sex constrain the flight speeds of central-place foraging albatrosses. *Ecol. Monogr.* **79**, 663-679. doi:10.1890/07-2111.1
- Wall, J., Douglas-Hamilton, I. and Vollrath, F. (2006). Elephants avoid costly mountaineering. *Curr. Biol.* **16**, R527-R529. doi:10.1016/j.cub.2006.06.049
- Weimerskirch, H., Guionnet, T., Martin, J., Shaffer, S. A. and Costa, D. P. (2000). Fast and fuel efficient? Optimal use of wind by flying albatrosses. *Proc. R. Soc. B* **267**, 1869-1874. doi:10.1098/rspb.2000.1223
- Weimerskirch, H., Louzao, M., De Grissac, S. and Delord, K. (2012). Changes in wind pattern alter albatross distribution and life-history traits. *Science* **335**, 211-214. doi:10.1126/science.1210270
- Williams, T. M., Friedl, W. A., Fong, M. L., Yamada, R. M., Sedivy, P. and Haun, J. E. (1992). Travel at low energetic cost by swimming and wave-riding bottlenose dolphins. *Nature* **355**, 821-823. doi:10.1038/355821a0
- Williams, H., Shepard, E. L. C., Duriez, O. and Lambertucci, S. A. (2015). Can accelerometry be used to distinguish between flight types in soaring birds? *Anim. Biotelemetry* **3**, 45. doi:10.1186/s40317-015-0077-0
- Williams, H., Holton, M., Shepard, E., Largey, N., Norman, B., Ryan, P. G., Duriez, O., Scantlebury, M., Quintana, F., Magowan, E. A. et al. (2017). Identification of animal movement patterns using tri-axial magnetometry. *Mov. Ecol.* **5**, 6. doi:10.1186/s40462-017-0097-x
- Wilmers, C. C., Nickel, B., Bryce, C. M., Smith, J. A., Wheat, R. E., Yovovich, V. and Hebblewhite, M. (2015). The golden age of bio-logging: how animal-borne sensors are advancing the frontiers of ecology. *Ecology* **96**, 1741-1753. doi:10.1890/14-1401.1
- Wilson, J. (1975). Sweeping flight and soaring by albatrosses. *Nature* **257**, 307-308. doi:10.1038/257307a0
- Wilson, R. P., White, C. R., Quintana, F., Halsey, L. G., Liebsch, N., Martin, G. R. and Butler, P. J. (2006). Moving towards acceleration for estimates of activity-specific metabolic rate in free-living animals: the case of the cormorant. *J. Anim. Ecol.* **75**, 1081-1090. doi:10.1111/j.1365-2656.2006.01127.x
- Wilson, J. W., Mills, M. G. L., Wilson, R. P., Peters, G., Mills, M. E. J., Speakman, J. R., Durant, S. M., Bennett, N. C., Marks, N. J. and Scantlebury, M. (2013a). Cheetahs, *Acinonyx jubatus*, balance turn capacity with pace when chasing prey. *Biol. Lett.* **9**, 20130620. doi:10.1098/rstb.2013.0620
- Wilson, R. P., Griffiths, I. W., Legg, P. A., Friswell, M. I., Bidder, O. R., Halsey, L. G., Lambertucci, S. A. and Shepard, E. L. C. (2013b). Turn costs change the value of animal search paths. *Ecol. Lett.* **16**, 1145-1150. doi:10.1111/ele.12149
- Wilson, R. P., Börger, L., Holton, M. D., Scantlebury, D. M., Gómez-Laich, A., Quintana, F., Rosell, F., Graf, P. M., Williams, H., Gunner, R. et al. (2020). Estimates for energy expenditure in free-living animals using acceleration proxies: a reappraisal. *J. Anim. Ecol.* **89**, 161-172. doi:10.1111/1365-2656.13040
- Yoda, K., Sato, K., Niizuma, Y., Kurita, M., Bost, C., Le Maho, Y. and Naito, Y. (1999). Precise monitoring of porpoising behaviour of Adelie penguins determined using acceleration data loggers. *J. Exp. Biol.* **202**, 3121-3126. doi:10.1242/jeb.202.22.3121